

loss of fluorescence for a given bouton was calculated as the difference between the average of 10 data points of baseline before a stimulus and the average of the last 10 data points of the time-lapse sequence.

Modelling. Exocytosis of releasable vesicles under a sustained stimulus was lumped into a single rate α (see Fig. 4a). In the fused state, dye could either depart with rate δ or be taken up again by means of fast endocytosis with rate β . Freshly endocytosed vesicles were recycled back to the readily releasable pool either with a single rate γ (Fig. 4b) or through a series of n consecutive steps, each having a rate constant γ/n (Fig. 4c). The variables S_x represent the relative amounts of dye incorporated into vesicle membrane pools, with subscripts 0, 1 and 2 denoting readily releasable, fused and retrieved vesicles. The state vector $\mathbf{S} = (S_0, S_1, S_2)^T$ represents the filling of the three states, and its evolution in time is described by the matrix equation

$$\frac{d\mathbf{S}}{dt} = \begin{bmatrix} -\alpha & 0 & \gamma \\ \alpha & -(\beta + \delta) & 0 \\ 0 & \beta & -\gamma \end{bmatrix} \mathbf{S}$$

with the sum of the states S_0 , S_1 and S_2 corresponding to the observable fluorescence. The amount of retrieved dye can be obtained by integrating the flux through the transition β (Fig. 4a, bottom).

Received 2 April; accepted 14 April 1998.

- Harris, K. M. & Sultan, P. Variation in the number, location and size of synaptic vesicles provides an anatomical basis for the nonuniform probability of release at hippocampal CA1 synapses. *Science* **266**, 1387–1395 (1995).
- Schikorski, T. & Stevens, C. F. Quantitative ultrastructural analysis of hippocampal excitatory synapses. *J. Neurosci.* **17**, 5858–5867 (1997).
- Betz, W. J., Mao, F. & Smith, C. B. Imaging exocytosis and endocytosis. *Curr. Opin. Neurobiol.* **6**, 365–371 (1996).
- Ryan, T. A., Smith, S. J. & Reuter, H. The timing of synaptic vesicle endocytosis. *Proc. Natl Acad. Sci. USA* **93**, 5567–5571 (1996).
- Cremona, O. & De Camilli, P. Synaptic vesicle endocytosis. *Curr. Opin. Neurobiol.* **7**, 323–330 (1997).
- Ryan, T. A. *et al.* The kinetics of synaptic vesicle recycling measured at single presynaptic boutons. *Neuron* **11**, 713–724 (1993).
- Liu, G. & Tsien, R. W. Properties of synaptic transmission at single hippocampal synaptic boutons. *Nature* **268**, 1624–1628 (1995).
- Wu, L. G. & Betz, W. J. Nerve activity but not intracellular calcium determines the time course of endocytosis at the frog neuromuscular junction. *Neuron* **17**, 769–779 (1996).
- Thomas, P., Lee, A. K., Wong, J. G. & Almers, W. A triggered mechanism retrieves membrane in seconds after Ca^{2+} -stimulated exocytosis in single pituitary cells. *J. Cell Biol.* **124**, 667–675 (1994).
- Smith, C. & Neher, E. Multiple forms of endocytosis in bovine adrenal chromaffin cells. *J. Cell Biol.* **139**, 885–894 (1997).
- Engisch, K. L. & Nowycky, M. Compensatory and excess retrieval: two types of endocytosis following single step depolarizations in bovine adrenal chromaffin cells. *J. Physiol. (Lond.)* **506**, 591–608 (1998).
- Henkel, A. W. & Almers, W. Fast steps in exocytosis and endocytosis studied by capacitance measurements in endocrine cells. *Curr. Opin. Neurobiol.* **6**, 350–357 (1996).
- Heuser, J. E. & Reese, T. S. Evidence for recycling of synaptic vesicle membrane during transmitter release at the frog neuromuscular junction. *J. Cell Biol.* **57**, 315–344 (1973).
- Miller, T. M. & Heuser, J. E. Endocytosis of synaptic vesicle membrane at the frog neuromuscular junction. *J. Cell Biol.* **98**, 685–698 (1984).
- Koenig, J. H. & Ikeda, K. Synaptic vesicles have two distinct recycling pathways. *J. Cell Biol.* **135**, 797–808 (1996).
- Ceccarelli, B. & Hurlbut, W. P. Ca^{2+} -dependent recycling of synaptic vesicles at the frog neuromuscular junction. *J. Cell Biol.* **87**, 297–303 (1980).
- Fesce, R., Grohovaz, E., Valtorta, F. & Meldolesi, J. Neurotransmitter release: fusion or “kiss and run”? *Trends Cell Biol.* **4**, 1–4 (1994).
- Henkel, A. W. & Betz, W. J. Staurosporine blocks evoked release of FM1-43 but not acetylcholine from frog motor nerve terminals. *J. Neurosci.* **15**, 8246–8258 (1995).
- Murthy, V. N. & Stevens, C. F. Synaptic vesicles retain their identity through the endocytotic cycle. *Nature* **392**, 497–501 (1998).
- Takei, K., Mundigl, O., Daniell, L. & De Camilli, P. The synaptic vesicle cycle: a single vesicle budding step involving clathrin and dynamin. *J. Cell Biol.* **133**, 1237–1250 (1996).
- Margaroli, A. & Tsien, R. W. Glutamate-induced long-term potentiation of the frequency of miniature synaptic currents in cultured hippocampal neurons. *Nature* **357**, 134–139 (1992).
- Lagnado, L., Gomis, A. & Job, C. Continuous vesicle cycling in the synaptic terminal of retinal bipolar cells. *Neuron* **17**, 957–967 (1996).
- Kraszewski, K., Daniell, L., Mundigl, O. & De Camilli, P. Mobility of synaptic vesicles in nerve endings monitored by recovery from photobleaching of synaptic vesicle-associated fluorescence. *J. Neurosci.* **16**, 5905–5913 (1996).
- Parsons, T. D., Lenzi, D., Almers, W. & Roberts, W. M. Calcium-triggered exocytosis and endocytosis in an isolated presynaptic cell: capacitance measurements in sacular hair cells. *Neuron* **13**, 875–883 (1994).
- Burgoyne, R. D. Fast exocytosis and endocytosis triggered by depolarisation in single adrenal chromaffin cells before rapid Ca^{2+} current run-down. *Pflügers Arch.* **430**, 213–219 (1995).
- Plattner, H., Braun, C. & Hentschel, J. Facilitation of membrane fusion during exocytosis and exocytosis-coupled endocytosis and acceleration of “ghost” detachment in *Paramecium* by extracellular calcium. A quenched-flow/freeze-fracture analysis. *J. Membr. Biol.* **158**, 197–208 (1997).
- von Gersdorff, H. & Matthews, G. Inhibition of endocytosis by elevated internal calcium in a synaptic terminal. *Nature* **370**, 652–666 (1994).
- Ramaswami, M., Krishnan, K. S. & Kelly, R. B. Intermediates in synaptic vesicle recycling revealed by optical imaging of *Drosophila* neuromuscular junctions. *Neuron* **13**, 363–375 (1994).
- Zimmerberg, J., Blumenthal, R., Sarkar, D. P., Curran, M. & Morris, S. J. Restricted movement of lipid and aqueous dyes through pores formed by influenza hemagglutinin during cell fusion. *J. Cell Biol.* **127**, 1885–1894 (1994).
- Betz, W. J. & Bewick, G. S. Optical monitoring of transmitter release and synaptic vesicle recycling at the frog neuromuscular junction. *J. Physiol. (Lond.)* **460**, 287–309 (1993).

Acknowledgements. We thank S. J. Smith and T. L. Schwarz for critically reading the manuscript, members of the Tsien laboratory for comments; and J. Bergsman for discussions and suggestions. This work was supported by grants from NIMH, the Mathers Charitable Foundation, the McKnight Endowment Fund for Neuroscience (R.W.T.), and fellowships from the Boehringer Ingelheim Fonds (J.K.) and the American Heart Association California Affiliate (E.T.K.).

Correspondence and requests for materials should be addressed to R.W.T. (e-mail: rwttsien@leland.stanford.edu).

Nitric oxide functions as a signal in plant disease resistance

Massimo Delledonne*†‡, Yiji Xia*‡§, Richard A. Dixon* & Chris Lamb*

* Plant Biology Laboratory, The Salk Institute, La Jolla, California 92037, USA

§ Plant Biology Division, The Noble Foundation, Ardmore, Oklahoma 73402, USA

‡ These authors contributed equally to this work.

Recognition of an avirulent pathogen triggers the rapid production of the reactive oxygen intermediates superoxide (O_2^-) and hydrogen peroxide (H_2O_2)¹. This oxidative burst drives cross-linking of the cell wall², induces several plant genes involved in cellular protection and defence^{3,4}, and is necessary for the initiation of host cell death in the hypersensitive disease-resistance response^{1,3}. However, this burst is not enough to support a strong disease-resistance response^{4,5}. Here we show that nitric oxide, which acts as a signal in the immune, nervous and vascular systems⁶, potentiates the induction of hypersensitive cell death in soybean cells by reactive oxygen intermediates and functions independently of such intermediates to induce genes for the synthesis of protective natural products. Moreover, inhibitors of nitric oxide synthesis compromise the hypersensitive disease-resistance response of *Arabidopsis* leaves to *Pseudomonas syringae*, promoting disease and bacterial growth. We conclude that nitric oxide plays a key role in disease resistance in plants.

The oxidative burst required for hypersensitive cell death in soybean cell suspensions inoculated with avirulent *P. syringae* pv. *glycinia* gives a sustained accumulation of 6–10 μM H_2O_2 (ref. 7). Addition of the H_2O_2 -generating system glucose (0.5 mM)/glucose oxidase (0.5 U ml⁻¹) to these cell suspensions resulted in a steady-state accumulation of ~6 μM H_2O_2 for >3 h, and hence closely mimics the oxidative burst induced by the avirulent pathogen. However, *in situ* generation of H_2O_2 in this fashion, or equivalent generation of O_2^- by addition of xanthine/xanthine oxidase, induced only a relatively weak cell-death response (Fig. 1a).

In the immune system, reactive oxygen intermediates (ROI) often function together with nitric oxide (NO), for example in macrophage killing of bacteria and tumour cells^{6,8}. We therefore tested whether NO might be the second factor required for a strong hypersensitive disease-resistance response (HR). Treatment of cell suspensions with 0.5 mM sodium nitroprusside generated a steady-state NO concentration of ~2 μM (see below), which in the absence of ROI did not induce cell death. However, this NO donor markedly potentiated the induction of cell death by exogenous H_2O_2 or O_2^- (Fig. 1a). The interaction was synergistic, with NO promoting a 5–10-fold increase in ROI-induced cell death. Potassium ferrocyanide, an analogue of sodium nitroprusside that does not release NO, had no effect on ROI-induced cell death.

NO also potentiated cell death induced by endogenous ROI. Activation of the oxidative burst following pathogen recognition involves a protein kinase cascade^{3,9}. Cantharidin, an inhibitor of

† Permanent address: Istituto di Genetica, Università Cattolica S.C., Piacenza, 29100 Italy.

type-2a protein phosphatases, partially activates this signalling pathway in the absence of pathogen avirulence factors³. Salicylic acid, which functions in signal amplification⁷, enhances this effect, resulting in the accumulation of >30 μM H_2O_2 (Fig. 2i; ref. 7). This massive oxidative burst caused only a weak induction of cell death, but simultaneous addition of nitroprusside strongly potentiated the response (Fig. 1a). Likewise, a yeast cell-wall elicitor, which rapidly stimulates a strong oxidative burst¹⁰ (Fig. 2j), did not induce cell death without exogenous NO (data not shown). Rapid agitation of plant cells also causes ROI production¹¹ and, under these conditions, which gave a steady-state H_2O_2 concentration of $\sim 1 \mu\text{M}$ in the soybean cultures, nitroprusside induced cell death without added ROI (Fig. 1b). This response was blocked not only by the NO scavenger 2-4-carboxyphenyl-4,4,5,5-tetramethylimidazole-

1-oxyl-3-oxide (CPTIO), but also by diphenylene iodonium, an inhibitor of the neutrophil NADPH oxidase that inhibits the plant oxidative burst³, and by catalase, which destroys H_2O_2 , thereby confirming the involvement of endogenous ROI together with the added NO (Fig. 1b). Two other NO donors, S-nitroso-N-acetylpenicillamine and diethylamino NO, gave a similar response (data not shown).

The synergistic interaction between exogenous NO and ROI suggested that NO might have a physiological function in the HR. Endogenous NO was assayed by the conversion of haemoglobin to methaemoglobin¹². ROI can interfere with this assay, and although haemoglobin conversion was observed with cells treated with yeast elicitor, pretreatment of the assay sample with superoxide dismutase plus catalase abolished this spurious signal (Fig. 2a). Neither yeast

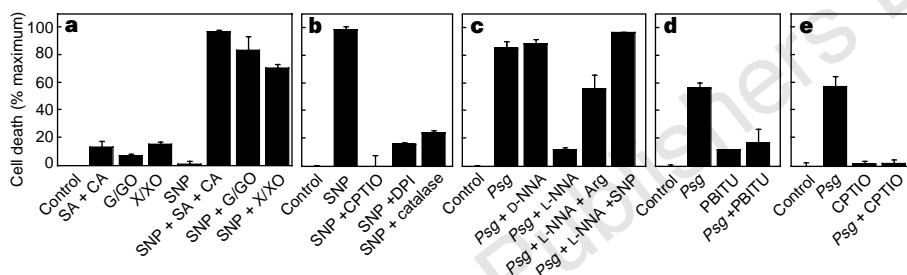


Figure 1 Function of NO in the induction of hypersensitive cell death in soybean cell suspension cultures. **a, b**, NO potentiation of ROI-induced cell death. **c, d**, NO function in *P. syringae* pv. *glycinea* (*Psg*)-induced hypersensitive cell death. In **b**, cell suspensions were rapidly agitated (100 r.p.m.) to stimulate ROI generation sufficient to maintain a steady-state H_2O_2 concentration of $\sim 1 \mu\text{M}$. In **a, c-e**, cell suspensions were shaken slowly (60 r.p.m.) and the basal level of H_2O_2 was $<0.05 \mu\text{M}$. Reagents were added as indicated at the following final concentrations:

50 μM salicylic acid (SA), 4 μM cantharidin (CA), 0.5 mM glucose + 0.5 U ml^{-1} glucose oxidase (G/GO), 0.5 mM xanthine + 0.5 U ml^{-1} xanthine oxidase (X/XO), 0.5 mM nitroprusside (SNP), 5 mM (**b**) and 50 μM (**d**) CPTIO, 10 μM diphenylene iodonium (DPI), 300 U ml^{-1} catalase, 200 μM L-NNA or D-NNA, 1 mM PBITU, 2 mM arginine. Cell death was assayed after 24 h by spectrophotometric determination of Evans blue uptake relative to that in equivalent cell suspensions killed by ethanol.

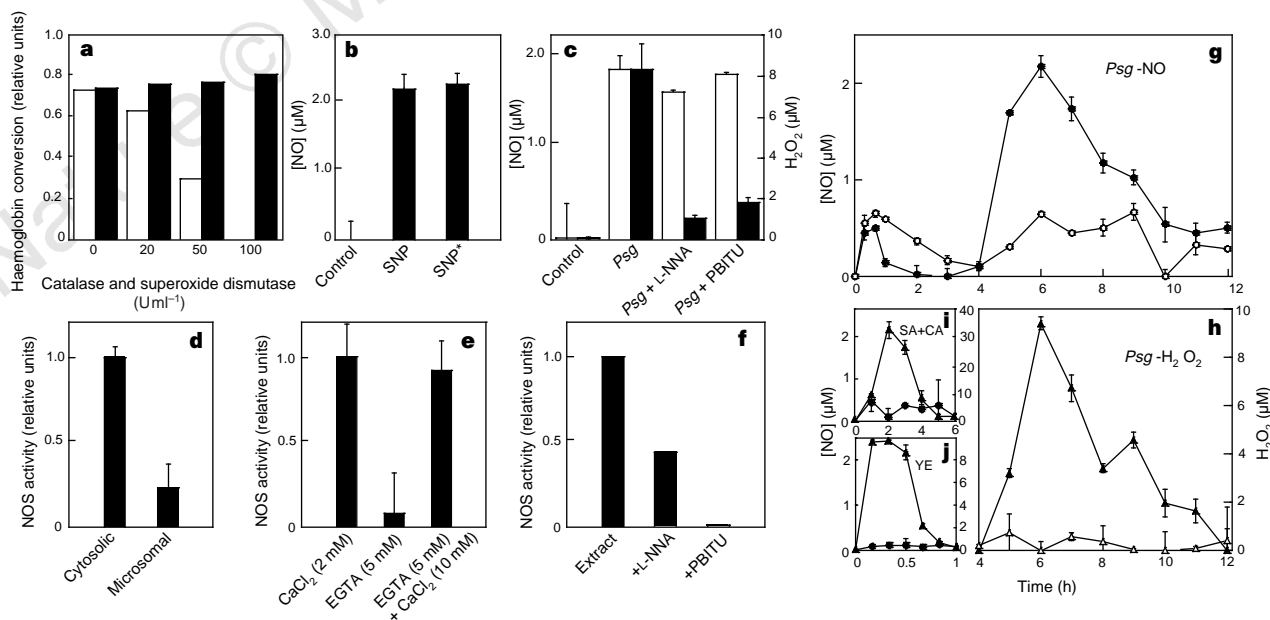


Figure 2 NO production in soybean cell suspensions. **a**, Validation of NO assay. The effects of pretreatment of assay samples with the indicated activities of superoxide dismutase and catalase on haemoglobin conversion were measured in samples from cells induced with yeast elicitor for 20 min (white bars) or *P. syringae* pv. *glycinea* (*Psg*) for 6 h (black bars). **b**, NO accumulation in cells 2 h after treatment with 0.5 mM nitroprusside (SNP). Asterisk denotes cells that were rapidly shaken to give mechanically induced accumulation of ROI. **c**, Effect of 0.2 mM L-NNA or 1 mM PBITU on *Psg* induction of H_2O_2 (white bars) and NO (black

bars) accumulation after 6 h. **d**, Distribution of NOS activity between cytosolic and microsomal fractions of soybean whole-cell extracts. Relative activities are presented on a cell-equivalent basis. **e**, Calcium dependence of cytosolic NOS activity. **f**, Effect of 0.2 mM L-NNA or 1 mM PBITU on NOS activity in whole-cell extracts. **g-j**, NO (circles) and H_2O_2 (triangles) accumulation in soybean cell suspensions treated with: **g, h**, *Psg* (filled symbols: avirulent strain; open symbols: isogenic virulent strain); **i**, cantharidin (CA, 1 μM) + salicylic acid (SA, 50 μM); **j**, yeast elicitor (YE, 100 μg glucose equivalents ml^{-1}).

elicitor nor salicylic acid plus cantharidin stimulated NO accumulation, as measured by haemoglobin assay after superoxide dismutase and catalase pretreatment (Fig. 2i, j), consistent with the inability of these stimuli to trigger cell death despite activation of a strong oxidative burst. In contrast, inoculation of soybean cell suspensions with *P. syringae* pv. *glycinea* stimulated NO production, as measured by assay of samples depleted for ROI by pretreatment with superoxide dismutase plus catalase (Fig. 2a, g). A rapid, relatively weak stimulation by both avirulent and virulent strains was followed by several-fold greater NO production specifically in cells inoculated with the avirulent strain, concomitant with the avirulence gene-dependent oxidative burst (Fig. 2g, h). The maximal accumulation of 2 μ M NO and of 10 μ M H₂O₂ closely matched their respective levels in the experiments with nitroprusside and glucose/glucose oxidase (Fig. 2b), and hence would be sufficient to account for the induction of hypersensitive cell death by avirulent *P. syringae*.

In animals, NO is generated by the reaction arginine → citrulline + NO, which is catalysed by NO synthase (NOS)⁶. Plants also have NOS activity^{13,14}, and in our soybean cell extracts NOS activity was calcium-dependent and found primarily in the cytosolic fraction (Fig. 2d, e). The NOS inhibitors N^ω-nitro-L-arginine (L-NNA) and S,S'-1,3-phenylene-bis(1,2-ethanediy)l-bis-isothiourea (PBITU)^{15,16}, which inhibits this reaction in soybean cell extracts (Fig. 2f), markedly inhibited (at concentrations comparable to those used with animal cells) the accumulation of endogenous NO in bacterially induced cells, but had no effect on the accumulation of H₂O₂ (Fig. 2c). Both PBITU and L-NNA, but not the inactive enantiomer D-NNA, blocked bacterial induction of hypersensitive cell death (Fig. 1c, d). L-NNA inhibition could be partially competed with exogenous arginine or completely bypassed with nitroprusside (Fig. 1c). Moreover, the induction of hypersensitive cell death by avirulent *P. syringae* was also inhibited by the NO scavenger CPTIO (Fig. 1e), which blocks NO accumulation by a different mechanism.

H₂O₂ drives oxidative crosslinking of tyrosine-rich cell-wall structural proteins² and the oxidative burst also induces protective cellular genes encoding glutathione S-transferase (*gst*) and glutathione peroxidase³. In soybean cells, however, ROI are not the primary signals for rapid induction of defence genes encoding enzymes of phenylpropanoid biosynthesis involved in the synthesis of antibiotics, lignin and salicylic acid¹⁵. Whereas L-NNA had little effect on the initial induction of *gst* by avirulent *P. syringae*, the accumulation of transcripts encoding phenylalanine ammonia-lyase (*pal*), the first enzyme of the phenylpropanoid pathway¹⁷, was markedly reduced (Fig. 3). Bacterial induction of transcripts

encoding chalcone synthase (*chs*), the first enzyme of the branch specific for flavonoids and isoflavonoid-derived antibiotics¹⁷, showed a similar dependence on endogenous NO (data not shown). Moreover, sodium nitroprusside caused a rapid induction of *pal* and *chs* transcripts that was blocked by CPTIO but not by catalase. In contrast, nitroprusside caused only a slow accumulation of *gst* transcripts and this was sensitive to catalase as well as to CPTIO (Fig. 3).

To test whether NO functions *in planta*, we examined the effects of inhibitors of NO accumulation in a genetically well defined host-pathogen interaction. Infiltration of leaves of *Arabidopsis* ecotype Col-0, which contains the *RPM1* resistance gene, with *P. syringae* pv. *maculicola* carrying the corresponding *avrRpm1* avirulence gene, results in a localized HR lesion which is first apparent ~1 d after inoculation¹⁸. Co-infiltration of the NOS inhibitors L-NNA or PBITU blocked this early HR and promoted the spreading chlorosis observed in the compatible interaction with the isogenic virulent bacteria lacking *avrRpm1* (Fig. 4a, b). L-NNA and PBITU alone did not cause disease symptoms (Fig. 4a) and had no effect on axenic bacterial growth (data not shown). Development of disease symptoms in leaves blocked for NO accumulation was accompanied by enhanced bacterial growth, although not to the extent seen with the isogenic virulent strain (Fig. 4c).

In the vertebrate native immune system, NO potentiates the antimicrobial and cytotoxic activities of ROI^{6,8}. We have shown by several independent approaches that NO also functions in the plant HR and appears to be critical for preventing pathogen spread from the inoculation site. Moreover, our results reveal a striking complementarity between NO and ROI signal functions, involving not only synergistic induction of hypersensitive cell death, but also independent activation of complementary gene sets. This arrangement provides for flexible deployment of specific defences and binary control of progression to hypersensitive cell death.

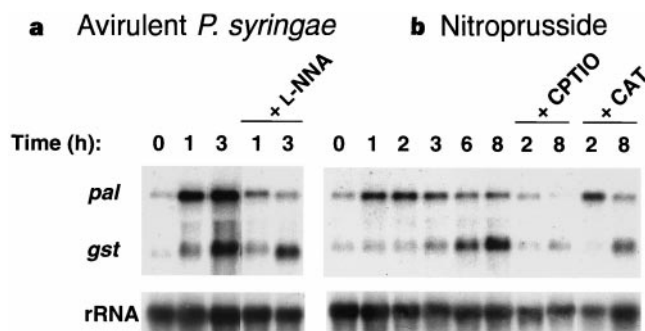


Figure 3 NO induction of *pal*. Northern blot analysis of **a**, the effects of the NO synthase inhibitor L-NNA on *pal* and *gst* induction by avirulent *P. syringae* pv. *glycinea*, and **b**, NO induction of *pal* and *gst*. RNA loading was checked by hybridization of rRNA. Reagents were added as indicated at the following final concentrations: 0.5 mM nitroprusside, 200 μ M L-NNA, 50 μ M CPTIO, 300 U ml⁻¹ catalase (CAT).

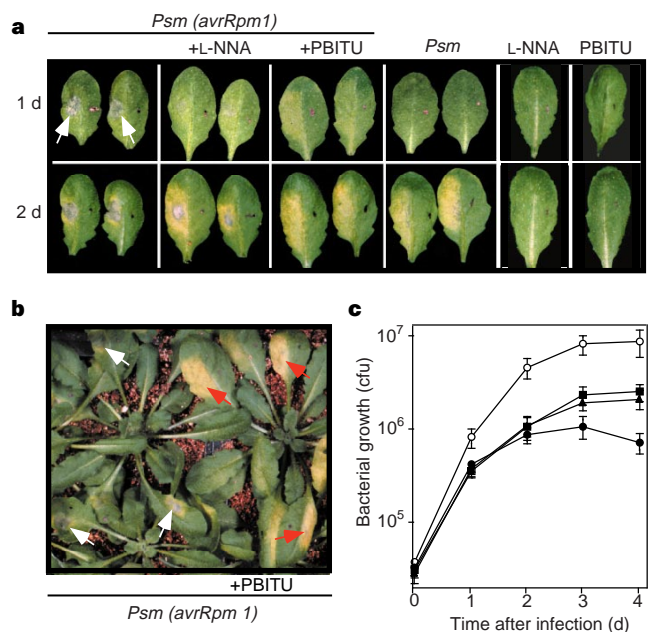


Figure 4 Function of NO in the hypersensitive disease-resistance response: effects of L-NNA and PBITU on: **a, b**, visible symptoms, and **c**, bacterial growth. *Psm* represents virulent *P. syringae* pv. *maculicola* (open circles); *Psm avrRpm1*, the isogenic avirulent strain of *P. syringae* pv. *maculicola* inoculated alone (filled circles), with L-NNA (triangles) or with PBITU (squares). PBITU was 1 mM in all experiments, L-NNA was 0.1 mM in **a**, 0.2 mM in **c**. Red arrows mark disease; white arrows, HR. In **c**, data points are the mean and standard deviation of three replicates, each from three leaf discs. These experiments were repeated three times with similar results.

In animals, many physiological effects of NO are mediated by cyclic GMP, following direct activation of guanylyl cyclase^{6,8}. In plants, cGMP functions in the phytochrome-mediated light induction of *chs* associated with the formation of phenylpropanoid-derived pigments¹⁹. Recent results indicate that cGMP also functions in the induction of *pal* by exogenous NO (ref. 29), associated with the synthesis of phenylpropanoid products with defence functions²⁰. Moreover, ROI induce hypersensitive cell death by raising cytosolic calcium²¹ and NO can reduce the threshold for calcium signalling by modulation of cGMP-gated ion channels²². Hence, NO may activate cGMP pathways for both defence gene induction and potentiation of ROI-induced cell death.

An enzyme system similar to the neutrophil NADPH oxidase apparently contributes to the oxidative burst in plants^{23,24}. Although NOS homologues have not yet been reported in plants, a plant complementary DNA sequence with pronounced similarity to PIN, a protein inhibitor of NOS, has been identified²⁵, suggesting that functional parallels between the native immune system and the plant HR may be maintained by conserved molecular mechanisms. □

Methods

Soybean (*Glycine max* cv. Williams 82) cell cultures, virulent *P. syringae* pv. *glycinea* race 4 and the isogenic strain carrying the *avrA* avirulence gene, which interacts with the soybean resistance gene *Rgm2* (ref. 26) were grown as described^{13,7}. Three days after subculture, aliquots of the soybean cell suspension were transferred to 12-well tissue-culture plates (1 ml per well) agitated at 60 or 100 r.p.m. Bacteria (10^8 colony forming units (CFU) per ml) and reagents at the indicated concentrations were added simultaneously as appropriate. The growth of *A. thaliana* ecotype Col-0, infiltration of leaves with virulent *P. syringae* pv. *maculicola* or the isogenic avirulent strain carrying *avrRpm1* ($5-10 \mu\text{l}$ of a bacterial suspension containing 5×10^6 CFU ml^{-1}), together with PBITU or L-NNA as indicated, and measurement of bacterial growth *in planta* have all been described²⁷.

Cell death was assayed by spectrophotometric measurement of the uptake of Evans blue stain⁷, and H₂O₂ accumulation by fluorescence determination of scopoletin destruction³. For NO assay, soybean cell suspensions were incubated with 100 U catalase and 100 U superoxide dismutase for 5 min to remove ROI before addition of oxyhaemoglobin ($5 \mu\text{M}$ final). After 2 min incubation, NO was quantified by spectrophotometric measurement of the conversion of oxyhaemoglobin to methaemoglobin¹². Each cell death, H₂O₂ and NO datum point is the mean and standard deviation of three to five replicates. NOS activity was assayed by the conversion of L-[³H]-arginine to L-[³H]-citrulline²⁸ in whole-cell extracts, and microsomal and cytosolic fractions²⁴. Northern blot hybridization was done as described³. Cantharidin, diphenylene iodonium, glucose oxidase and PBITU were from Calbiochem; CPTIO, diethylamino NO, S-nitroso-N-acetylpenicillamine were from Molecular Probes; all other reagents and enzymes were from Sigma.

Received 5 December 1997; accepted 1 June 1998.

- Lamb, C. & Dixon, R. A. The oxidative burst in plant disease resistance. *Annu. Rev. Plant Physiol. Plant Mol. Biol.* **48**, 251–275 (1997).
- Bradley, D. J., Kjellbom, P. & Lamb, C. J. Elicitor- and wound-induced oxidative cross-linking of a proline-rich plant cell wall protein: A novel, rapid defense response. *Cell* **70**, 21–30 (1992).
- Levine, A., Tenhaken, R., Dixon, R. A. & Lamb, C. H₂O₂ from the oxidative burst orchestrates the plant hypersensitive response. *Cell* **79**, 583–593 (1994).
- Jaobs, T., Tschöpe, M., Colling, C., Hahlbrock, K. & Scheel, D. Elicitor-stimulated ion fluxes and O₂⁻ from the oxidative burst are essential components in triggering defense gene activation and phytoalexin synthesis in parsley. *Proc. Natl Acad. Sci. USA* **94**, 4800–4805 (1997).
- Glazener, J. A., Orlandi, E. W. & Baker, J. C. The active oxygen response of cell suspensions is not sufficient to cause hypersensitive cell death. *Plant Physiol.* **110**, 759–763 (1996).
- Schmidt, H. H. W. & Walter, U. NO at work. *Cell* **78**, 919–925 (1994).
- Shirasu, K., Nakajima, H., Rajasekhar, V. K., Dixon, R. A. & Lamb, C. Salicylic acid potentiates an agonist-dependent gain control that amplifies pathogen signals in the activation of defense mechanisms. *Plant Cell* **9**, 261–270 (1997).
- Nathan, C. Natural resistance and nitric oxide. *Cell* **82**, 873–876 (1995).
- Chandra, S., Martin, G. B. & Low, P. S. The Pto kinase mediates a signaling pathway leading to the oxidative burst in tomato. *Proc. Natl Acad. Sci. USA* **93**, 13393–13397 (1996).
- Guo, Z.-J. & Ohta, Y. Effect of ethylene biosynthesis on the accumulation of 6-methoxymellein induced by elicitors in carrot cells. *J. Plant Physiol.* **144**, 700–704 (1994).
- Yahraus, T., Chandra, S., Legendre, L. & Low, P. S. Evidence for a mechanically induced oxidative burst. *Plant Physiol.* **109**, 1259–1266 (1995).
- Murphy, M. E. & Noack, E. Nitric oxide assay using hemoglobin method. *Meth. Enzymol.* **233**, 241–250 (1994).

- Cueto, M. *et al.* Presence of nitric oxide synthase activity in roots and nodules of *Lupinus albus*. *FEBS Lett* **398**, 159–164 (1996).
- Ninnemann, H. & Maier, J. Indications for the occurrence of nitric oxide synthases in fungi and plants and the involvement in photocondensation of *Neurospora crassa*. *Photochem. Photobiol.* **64**, 393–398 (1996).
- Griffith, O. W. & Stuehr, D. J. Nitric oxide synthases: Properties and catalytic mechanism. *Annu. Rev. Physiol.* **57**, 707–736 (1995).
- Garvey, E. P. *et al.* Potent and selective inhibition of human nitric oxide synthases. *J. Biol. Chem.* **269**, 26669–26676 (1994).
- Dixon, R. A. & Paiva, N. Stress-induced phenylpropanoid metabolism. *Plant Cell* **7**, 1085–1097 (1995).
- Debener, T., Lehnackers, H., Arnold, M. & Dangel, J. L. Identification and molecular mapping of a single *Arabidopsis thaliana* locus determining resistance to a phytopathogenic *Pseudomonas syringae* isolate. *Plant J.* **1**, 289–302 (1991).
- Bowler, C., Neuhaus, G., Yamagata, H. & Chua, N.-H. Cyclic GMP and calcium mediate phytochrome phototransduction. *Cell* **77**, 73–81 (1994).
- Noritake, T., Kawakita, K. & Doke, N. Nitric oxide induces phytoalexin accumulation in potato tuber tissues. *Plant Cell Physiol.* **37**, 113–116 (1996).
- Levine, A., Pennell, R. I., Alvarez, M. E., Palmer, R. & Lamb, C. Calcium-stimulated apoptosis in a plant hypersensitive disease resistance response. *Curr. Biol.* **6**, 427–437 (1996).
- Berridge, M. J. A tale of two messengers. *Nature* **365**, 388–389 (1993).
- Groom, Q. J. *et al.* *rbh1A*, a rice homologue of the mammalian gp91^{phox} respiratory burst oxidase gene. *Plant J.* **10**, 515–522 (1996).
- Keller, T. *et al.* A plant homolog of the neutrophil NADPH oxidase gp91^{phox} subunit gene encodes a plasma membrane protein with Ca²⁺-binding domains. *Plant Cell* **10**, 255–266 (1998).
- Jaffrey, S. R. & Snyder, S. H. PIN: an associated protein inhibitor of neuronal nitric oxide synthase. *Science* **274**, 774–777 (1996).
- Keen, N. T. & Buzzell, R. I. New disease resistance genes in soybean against *Pseudomonas syringae* pv. *glycinea*: Evidence that one of them interacts with a bacterial elicitor. *Theor. Appl. Genet.* **81**, 133–138 (1991).
- Cameron, R. K., Dixon, R. A. & Lamb, C. J. Biologically induced systemic acquired resistance in *Arabidopsis thaliana*. *Plant J.* **5**, 715–725 (1994).
- Hevel, J. M. & Marletta, M. A. Nitric oxide synthase assays. *Meth. Enzymol.* **23**, 251–258 (1994).
- Durner, J., Wendehenne, D. & Klessig, D. F. Defense gene induction in tobacco by nitric oxide, cyclic GMP and cyclic ADP ribose. *Proc. Natl Acad. Sci. USA* (in the press).

Acknowledgements. Y.X. is a Noble/Salk postdoctoral fellow. This research was supported by grants to M.D. and C.L. from the Italian National Research Council and the Noble Foundation, respectively.

Correspondence and requests for materials should be addressed to C.L. (e-mail: lamb@salk.edu).

Transformation of primary human endothelial cells by Kaposi's sarcoma-associated herpesvirus

Ornella Flore*†, Shahin Rafii‡, Scott Ely*, John J. O'Leary*§, Elizabeth M. Hyjek* & Ethel Cesarman*

* Department of Pathology, † Division of Hematology–Oncology, Department of Medicine, Cornell University Medical College, New York, New York 10021, USA

† Dipartimento di Medicina Interna, Università di Cagliari, Cagliari, 09100, Italy

§ Departments of Pathology, The Coombe Women's Hospital and St James's Hospital Dublin, and Trinity College Dublin, Ireland

Kaposi's sarcoma-associated herpesvirus (KSHV), or human herpesvirus 8, is invariably present in Kaposi's sarcoma lesions^{1,2}. KSHV contains several viral oncogenes and serological evidence suggests that KSHV infection is necessary for the development of Kaposi's sarcoma, but cellular transformation by this virus has not so far been demonstrated. KSHV is found in the microvascular endothelial cells in Kaposi's sarcoma lesions and in the spindle 'tumour' cells^{3,4}, which are also thought to be of endothelial origin. Here we investigate the biological consequences of infecting human primary endothelial cells with purified KSHV particles. We find that infection causes long-term proliferation and survival of these cells, which are associated with the acquisition of telomerase activity and anchorage-independent growth. KSHV was present in only a subset of cells, and paracrine mechanisms were found to be responsible for the survival of uninfected cells. Their survival may have been mediated by upregulation of a receptor for vascular endothelial growth factor. Our results indicate that transformation of endothelial cells by KSHV, as